Available online at www.sciencedirect.com
SCIENCE DIRECT®
Scripta Materialia 51 (2004) 745–749
Scripta MATERIALIA
www.actamat-journals.com

# Linear coefficients of thermal expansion of $Au_{0.5}Ni_{0.5}Sn_4$, $Au_{0.75}Ni_{0.25}Sn_4$, and $AuSn_4$

Susan Pitely [a], Lubov Zavalij [a], Sergei Zarembo [b], Eric J. Cotts [a,*]

[a] Department of Physics and Materials Science Program, Binghamton University-SUNY, Science 2, P.O. Box 6000, Binghamton, NY 13902, USA
[b] Institute for Materials Research and Department of Chemistry, Binghamton University-SUNY, Binghamton, NY 13902, USA

Received 21 November 2003; accepted 13 February 2004
Available online 8 July 2004

**Abstract**

Linear coefficients of thermal expansion for $Au_{1-x}Ni_xSn_4$ and $AuSn_4$ alloys have been measured by thermo-mechanical analysis at temperatures between 340 and 460 K. These values are compared to those of other constituents of Ni/Au/PbSn solder joints. These joints have previously been shown to crack during thermal cycling in this temperature range.


*Keywords:* Pb-free solders; Mechanical properties; Intermetallic compounds; Annealing; Scanning electron microscopy

## 1. Introduction

Upon reflow of solder on a metallization, new intermetallic alloys grow at the solder/metallization interface. For instance, for Cu metallizations $Cu_6Sn_5$ with some $Cu_3Sn$ forms at the Sn/Cu interface [1–3]. If these alloy layers are too thick, they have deleterious effects on the mechanical reliability of the joints. Therefore, over the years the composition of electronic leads has changed from a single metal, usually Cu, to multi-layered structures with two or more metallic layers on top of each other. A thin coating of a noble metal such as Au is frequently used to protect the surface from oxidation, while a second layer, commonly Ni, is used as a diffusion barrier to prevent the Cu underneath it from interacting with solder. A number of investigators have shown that Ni/solder intermetallics grow more slowly than Cu/solder intermetallics during reflow [4–6].

The introduction of metals such as Au and Ni, which diffuse at very high rates in solder, and the reduction of the dimensions of the solder joints have dramatically altered the mechanisms of formation of solder alloys. For example, Au dissolves very quickly into molten Pb–Sn solder (1.33 μm/s) during reflow [7], and if present in concentrations above the solubility limit, it combines with Sn to form $AuSn_4$ precipitates upon cooling, which are dispersed in the solder. In a study of Pb–Sn solder joints reflowed on Au/Ni metalizations, Mei et al. [8] reported that during long term aging (336 h at 150° C) Au–Sn alloys form at the solder/$Ni_3Sn_4$ interface and degrade the strength of the joints. Other studies of similar systems [9–12] with lower Au concentrations (less than 0.34 versus 1.5 at.% for Mei et al.) also found that Au diffuses back to the PbSn solder/$Ni_3Sn_4$ interface. It was found that at this interface, Au combines with Ni and Sn to form a ternary phase of nominal composition $Au_{0.5}Ni_{0.5}Sn_4$ [9–12]. Thus it is found that even very low concentrations of Au in the joint might have a considerable effect on both the microstructure of the joint and the formation of different solder alloys, and thus the reliability of the solder interconnect.

While failures in Ni/Au/PbSn solder joints have been directly correlated with the formation of $Au_{1-x}Ni_xSn_4$ alloys at PbSn solder/$Ni_3Sn_4$ interfaces, the mechanism for this failure is not yet clearly understood. A careful characterization of the coefficients of thermal expansion of the materials in a solder joint contributes to an understanding of failures due to thermal cycling. The coefficients of thermal expansion have been previously measured for $Ni_3Sn_4$, and for PbSn solders, but not for $(AuNi)Sn_4$. Therefore, the thermal expansion of $Au_{1-x}Ni_xSn_4$ alloys was examined.

* Corresponding author. Tel.: +1-607-777-4371; fax: +1-607-777-6841.
*E-mail address:* ecotts@binghamton.edu (E.J. Cotts).

1359-6462/$ - see front matter 
doi:10.1016/j.scriptamat.2004.02.023

## 2. Experimental technique

### 2.1. Sample preparation and characterization

Samples with nominal compositions corresponding to $Au_{0.5}Ni_{0.5}Sn_4$, $Au_{0.75}Ni_{0.25}Sn_4$, and $AuSn_4$ were prepared by arc-melting stoichiometric mixtures of constituent elements (99.99% metals basis, Alfa Products) on a water-cooled copper hearth in a Ti-gettered argon atmosphere. Total sample masses were between 1 and 1.5 g. After initial melting and mixing the constituents, the resulting ingots were turned on their sides and re-melted at least once. Weight losses after the arc melting were less than 1 wt.%. The ingots were then annealed in evacuated silica-glass ampoules at $490 \pm 5$ K for time periods of 240–790 h. After annealing, the ingots, while still in the ampoules, were quenched in an ice water bath, removed from the ampoules, and then cut into two uneven pieces by a diamond wheel. The smaller pieces were characterized, as described below, to select homogeneous single phase samples. When found to be a single phase, the remaining bigger pieces of the as-cast ingots were machined to geometry with two parallel faces, and linear coefficients of thermal expansion (CTE) of the polycrystalline, single phase samples were determined by means of thermo-mechanical analysis (TMA).

Compositional, structural and thermal analysis of the $Au_{0.5}Ni_{0.5}Sn_4$, $Au_{0.75}Ni_{0.25}Sn_4$, and $AuSn_4$ samples before and after linear CTE measurements was performed by means of differential scanning calorimetry (DSC), powder and single crystal X-ray diffraction, optical metallography and scanning electron microscopy in WDA (wavelength dispersive analysis) mode [13]. All of these techniques indicated that the samples were single phase.

Previous results for the structural analysis indicated that nickel atoms substitute for gold atoms in the $AuSn_4$ structure to produce compounds isotypical with the pure $AuSn_4$ phase (the $PtSn_4$ structure type). Crystal structure refinement from powder data using the Rietveld method yielded lattice constants for two alloys of composition $Au_{1-x}Ni_xSn_4$ with $x = 0.25$ and 0.50, yielding $Au_{0.73}Ni_{0.27}Sn_4$ (space group $Ccca$, $a = 6.448$ Å, $b = 11.606$ Å, $c = 6.441$ Å) and $Au_{0.51}Ni_{0.49}Sn_4$ (space group $Ccca$, $a = 6.424$ Å, $b = 11.522$ Å, $c = 6.384$ Å). A single crystal X-ray diffraction experiment was performed for a compound $Au_{0.91}Ni_{0.09}Sn_4$ (space group $Ccca$, $a = 6.523$, $b = 11.676$, $c = 6.485$ Å). The results have been described in detail in our previous report [13].

Based upon previous electron microprobe analyses of the $Au_{1-x}Ni_xSn_4$ and $AuSn_4$ samples annealed for 400 h at $490 \pm 5$ K, it was expected that metallic Sn would be the only secondary phase present in the samples. The DSC was employed to check for presence of metallic Sn in the portions of the $Au_{1-x}Ni_xSn_4$ and $AuSn_4$ samples cleaved from the as-cast ingots. Due to its high heat flow sensitivity the DSC is capable of detecting a melting transition of small amounts of a substance, which translates to a detection limit of ca. 0.05 wt.% of metallic Sn for the DSC samples in this study. A DSC scan between 423 and 723 K with a heating rate of 10 K/min was performed for all the samples chosen for CTE measurements. None of them showed indication of melting of free metallic tin. The DSC data were supplemented by optical metallography and X-ray powder diffraction in the process of screening out single phase $Au_{1-x}Ni_xSn_4$ samples chosen for CTE measurements.

### 2.2. CTE measurements by thermo-mechanical analysis

Measurements of the linear CTEs (14,15) of each sample or reference material were performed in a thermal mechanical analyzer (TMA), model 2940, TA Instruments [16], interfaced to a PC for data acquisition and data analysis. The instrument measures elongation of a sample, placed between a glass probe and glass stage as a function of temperature of the sample, compression force applied to the sample, and time. The measurements were performed in expansion mode with applied force of 50 mN [16]. Dry nitrogen gas was flowed through the TMA furnace at the rate of 100 ml/min.

Cell and force calibrations of the TMA 2940 were performed as described in the instrument manual [16]. One-point temperature calibration of the instrument was performed using high-purity indium metal as a standard material (melting point 429.71 K, 99.99% metals basis, Alfa Products). An indium sample was placed under the expansion glass probe exerting compression force of 100 mN, and melting temperature of the standard was detected. Corresponding temperature correction (i.e. difference between the observed melting temperature and the melting point of indium metal) was applied to a calibration table in the data acquisition software of the instrument. After the temperature correction had been applied, another indium standard was tested in the instrument, and the deviation from the reference melting temperature was observed to be within 1 K. The temperature calibration routine was performed at least once a month during the CTE measurements.

The $Au_{1-x}Ni_xSn_4$ samples were cleaved from original as-cast ingots and machined to geometry with two parallel faces. The bottom side of the sample formed by cutting with a diamond wheel was lapped true using a fine india oilstone. To create a surface parallel to the bottom one, a surface grinding machine was used. The surface grinder removed material in small increments until the newly formed flat and parallel surface on top of the sample exhibited the area required for testing. The height of the samples varied between 4 and 5 mm.

Mean linear CTEs of the $Au_{1-x}Ni_xSn_4$ samples and two standard reference materials (SRMs) (obtained from National Institute of Standards and Technology,

NIST, [17,18]) were measured by a so-called interrupted heating method. In this method, a measured sample is slowly heated from one selected temperature to another and then kept isothermically at the higher temperature for a relatively long time. Dilation data are collected during the last portion of the isotherm, when the sample is considered to be in the state of quasi-thermal equilibrium with the furnace. In this study, a typical TMA procedure included a 5 K/min temperature ramp between 340 and 460 K interspersed with 60–75 min isotherms at 20 K intervals. It typically took between 7 and 8 h for a single run to be completed. During the measurement series, the samples and NIST standards were neither removed from nor repositioned on the TMA glass stage between test runs until all the scheduled runs for a sample or a standard were completed. Since the $AuSn_4$ is a metastable phase at room temperature, the temperature of $AuSn_4$ samples was maintained above 338 K at all times after the initial scan in the TMA.

The TMA 2940 was calibrated through examination of two NIST SRMs: copper (NIST SRM 736, [17]) and stainless steel (NIST SRM AISI 446, [18]). Mean linear CTEs were measured as a function of temperature for each SRM. A correction factor for each experimental temperature was calculated by dividing an accepted NIST linear CTE value by a corresponding experimentally measured CTE value for the standard. At least three different samples for each stoichiometry ($Au_{0.5}Ni_{0.5}Sn_4$, $Au_{0.75}Ni_{0.25}Sn_4$, and $AuSn_4$) were tested, each no less than 10 times. Averages were computed using the data from all of the runs, except for the first one, which was discarded in successive data analysis.

Mean linear coefficients of thermal expansion, $\alpha_I$, were calculated at median temperatures, $T_m = (T_1 + T_2)/2$ as

$$\alpha_I = \frac{L_2 - L_1}{L_{293}(T_2 - T_1)}$$

where $L_1$, $L_2$, and $L_{293}$ are the measured lengths of a sample at temperatures $T_1$, $T_2$, and 293 K, respectively [14,15].

## 3. Results and discussion

Tables 1 and 2 list the average linear coefficients of thermal expansion for the two NIST standards as a function of temperature as measured by means of the TMA-2940. The values were compared to the accepted NIST values [17,18], also included in Tables 1 and 2. Deviation from the NIST values was within 4% for the majority of the data (see Fig. 1). Table 3 lists the correction factors for both of the standards as a function of temperature along with the average factors, which were used to correct the experimental dilation data for the $Au_{1-x}Ni_xSn_4$ samples. The experimentally measured values of linear coefficients of thermal expansion for $Au_{0.5}Ni_{0.5}Sn_4$, $Au_{0.75}Ni_{0.25}Sn_4$, and $AuSn_4$ as a function of temperature are listed in Table 4. The corrected values are summarized in Table 5 and showed also in Fig. 2

Table 1
Linear CTEs measured for copper standard (NIST SRM736 L1). The accepted NIST values are also listed

| Temperature (K) | Average experimental CTEs (ppm/K) for copper | NIST accepted CTEs (ppm/K) [17] |
|---|---|---|
| 340 | 16.85 | 17.07 |
| 360 | 16.90 | 17.22 |
| 380 | 17.02 | 17.38 |
| 400 | 17.08 | 17.53 |
| 420 | 17.18 | 17.68 |
| 440 | 17.28 | 17.82 |
| 460 | 17.48 | 17.97 |
| 480 | 17.57 | 18.11 |
| 500 | 17.75 | 18.25 |
| 520 | 17.69 | 18.39 |
| 540 | 17.88 | 18.53 |

Table 2
Linear CTEs measured for stainless steel standard (NIST SRM 738 L1). The accepted NIST values are also listed

| Temperature (K) | Average experimental CTEs (ppm/K) for stainless steel | NIST accepted CTEs (ppm/K) [18] |
|---|---|---|
| 340 | 9.79 | 10.04 |
| 380 | 9.96 | 10.28 |
| 420 | 10.15 | 10.52 |
| 460 | 10.36 | 10.76 |
| 500 | 10.56 | 11.00 |
| 540 | 10.73 | 11.23 |
| 580 | 10.89 | 11.47 |

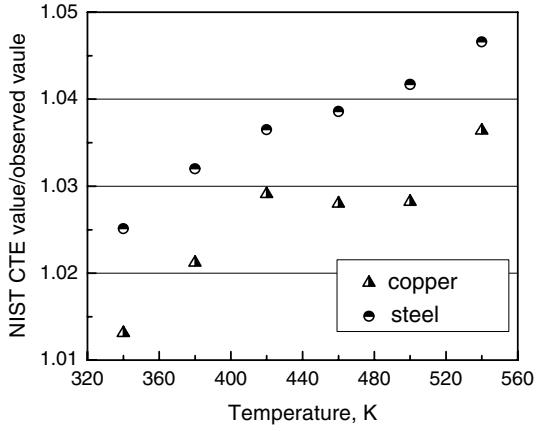


Fig. 1. Discrepancies observed between the measured linear CTEs for NIST standards (copper and stainless steel) and accepted NIST values for the standards. Data is shown as a quotient of an accepted NIST value divided by a corresponding measured value for a standard material.

Table 3
Correction factors calculated by dividing accepted NIST CTE values by the average experimentally measured CTE values

| Temperature (K) | Copper | Stainless steel | Average correction factor |
|---|---|---|---|
| 340 | 1.013 | 1.025 | 1.019 |
| 380 | 1.021 | 1.032 | 1.027 |
| 420 | 1.029 | 1.037 | 1.033 |
| 460 | 1.028 | 1.039 | 1.034 |
| 500 | 1.028 | 1.042 | 1.035 |
| 540 | 1.036 | 1.047 | 1.042 |

The average of the two was then taken to provide the average correction factor for any experimental dilation value at that temperature.

Table 4
Experimental linear CTEs for $Au_{0.5}Ni_{0.5}Sn_4$, $Au_{0.75}Ni_{0.25}Sn_4$, and $AuSn_4$ as measured in the TMA-2940

| Temperature (K) | Average experimental CTE values (ppm/K) for $Au_{0.5}Ni_{0.5}Sn_4$ | Average experimental CTE values (ppm/K) for $Au_{0.75}Ni_{0.25}Sn_4$ | Average experimental CTE values (ppm/K) for $AuSn_4$ |
|---|---|---|---|
| 340 | $18.3 \pm 1.3$ | $19.6 \pm 1.9$ | No data |
| 380 | $18.9 \pm 0.4$ | $20.1 \pm 1.6$ | $18.9 \pm 0.5$ |
| 420 | $19.3 \pm 0.4$ | $20.4 \pm 1.6$ | $19.6 \pm 0.6$ |
| 460 | $19.8 \pm 0.8$ | $21.0 \pm 0.9$ | $20.1 \pm 0.5$ |

Table 5
Linear CTEs for $Au_{0.5}Ni_{0.5}Sn_4$, $Au_{0.75}Ni_{0.25}Sn_4$, and $AuSn_4$ (shown also in Fig. 2)

| Temperature (K) | Linear CTEs (ppm/K) for $Au_{0.5}Ni_{0.5}Sn_4$ | Linear CTEs (ppm/K) for $Au_{0.75}Ni_{0.25}Sn_4$ | Linear CTEs (ppm/K) for $AuSn_4$ |
|---|---|---|---|
| 340 | $18.6 \pm 1.3$ | $19.9 \pm 1.9$ | No data |
| 380 | $19.3 \pm 0.4$ | $20.5 \pm 1.6$ | $19.3 \pm 0.5$ |
| 420 | $19.8 \pm 0.4$ | $20.9 \pm 1.7$ | $20.1 \pm 0.6$ |
| 460 | $20.3 \pm 0.8$ | $21.5 \pm 0.9$ | $20.6 \pm 0.5$ |

These corrected values were obtained by multiplying experimental values (Table 4) by the average correction factors (from Table 3).

along with accepted literature values for Ni, Au, and Sn metals [15].

The total uncertainty of the measurements was estimated based upon the variation in sample and reference measurements. For the $AuSn_4$ and $Au_{0.5}Ni_{0.5}Sn_4$ samples the error was estimated to be between 2 and 4% depending on temperature, which is consistent with previous measurements of the linear CTE of solder alloys. For the $Au_{0.75}Ni_{0.25}Sn_4$ samples the uncertainty was estimated to be appreciably higher, up to 7% at some temperatures, due to significant variations of the measured linear CTEs from sample to sample. Absolute uncertainties of the CTE data for the $Au_{1-x}Ni_xSn_4$ samples are summarized in Table 5.

The measured values of CTE for $Au_{0.5}Ni_{0.5}Sn_4$ and $AuSn_4$ are essentially the same over the temperature range from 380 to 460 K, while the measured values of

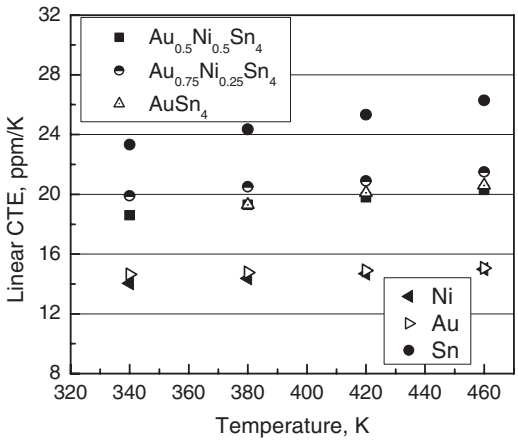


Fig. 2. Linear CTEs for $Au_{0.5}Ni_{0.5}Sn_4$, $Au_{0.75}Ni_{0.25}Sn_4$, and $AuSn_4$ (see also Table 5). Literature data for Ni, Au, and Sn metals [15] are also shown.

CTE for $Au_{0.75}Ni_{0.25}Sn_4$ are ca. 10% higher. $Au_{0.5}Ni_{0.5}Sn_4$ has been identified as the intermetallic compound found between $Ni_3Sn_4$ and Sn in joints prone to mechanical failure. The value of linear CTE for $Au_{0.5}Ni_{0.5}Sn_4$ at a temperature of 380 K was found to be 19.3 ppm/K (Table 5). This value can be compared to those for either Sn (24.3 ppm/K) or Ni (14.4 ppm/K) at this temperature [15]. The coefficients of thermal expansion for Pb–Sn solders depend on their composition, ranging from 20 to 29 ppm/K.

The differences (up to 25%) between the values of CTE for the alloy $Au_{0.5}Ni_{0.5}Sn_4$ and other metals in the joint are similar to those for other solder alloys commonly found in solder joints. For instance, the solder alloy $Ni_3Sn_4$ has a CTE of 15 ppm/K at 380 K [19]. These joints are reliable, although the difference in CTEs between PbSn and $Ni_3Sn_4$ is approximately 10 ppm/K. In another example, $Cu_3Sn$ and $Cu_6Sn_5$ (the solder alloys found in Cu/Sn and Cu/PbSn joints) both have CTE values of around 19 ppm/K at 380 K [19]. This is similar to the CTE value for $Au_{0.5}Ni_{0.5}Sn_4$, 19.3 ppm/K, while Cu has a CTE value of 17 ppm/K at this temperature [19].

For similar thicknesses of solder alloys, these other solder joints (Cu/$Cu_3Sn$/$Cu_6Sn_5$/PbSn and Ni/$Ni_3Sn_4$/PbSn) have been quite reliable. This is the case, even though the mismatch in CTEs is larger for some of these combinations than for those found in Ni/$Ni_3Sn_4$/$Au_{0.5}Ni_{0.5}Sn_4$/PbSn solder joints. While $Au_{0.5}Ni_{0.5}Sn_4$ has a clear detrimental effect on the reliability of solder joints, the underlying cause of these problems is probably not simply the mismatch of thermal expansive behaviors between them and surrounding metals or alloys. Their effects must be from a more intrinsic structural property of the alloy. Possibly poor adhesion to their neighbors, or excessive brittleness from their structure could be responsible for their ability to

undermine a solder's strength. More studies should be undertaken to determine their strength as compared to other intermetallics and their crystalline structure.

## Acknowledgments

We gratefully acknowledge the National Science Foundation for financial support (NSF DMI-0218129).

## References

[1] Kim HK, Tu KH. Phys Rev B 1996;53:16027.
[2] Zuruzi AS, Chiu CH, Lahiri SK, Chua KM. J Electron Mater 1999;28:1224.
[3] Schaefer M, Laub W, Fournelle RA, Liang J. Evaluation of intermetallic phase formation and concurrent dissolution of intermetallic during reflow soldering, Design and reliability of solders and solder interconnections. The Min, Metals Mater Soc 1997:247–57.
[4] Ghosh G. J Appl Phys 2000;88:6887.
[5] Ho CE, Chen WT, Kao CR. J Electronic Mater 2001;30(4): 379.
[6] Pan T, Blair HD, Nicholson JM, Oh S. EEP Adv Electron Packaging 1997;19(2):1347.
[7] Bader WG. Weld J: Res Suppl 1969;48(12):551s.
[8] Mei Z, Kauffmann M, Eslambolchi A, Johnson P. Proceedings of 48th Electronic Components and Technology Conference (Cat. No. 98CH36206), IEEE; 1998. p. 952.
[9] Zribi A., Chromik RR, Presthus R, Clum J, Teed K, Zavalij L, DeVita J, Tova J, Cotts EJ. IEEE 1999 Electronic Components and Technology Conference. 1999: p. 451.
[10] Zribi A, Chromik RR, Presthus R, Teed K, Zavalij L, DeVita J, et al. Solder metallization interdiffusion in microelectronic interconnects. IEEE CPMT 2000;23:383.
[11] Minor M, Morris Jr JW. Metall Mater Trans 2000;31A:798.
[12] Ho CE, Zheng R, Luo GL, Lin AH, Kao CR. J Electronic Mater 2000;29:1175.
[13] Zavalij L, Zribi A, Chromik RR, Pitely S, Zavalij PY, Cotts EJ. J Alloys Comp 2002;334:79.
[14] Taylor RE. In: Ho CY, editor. Thermal expansion of solids. CINDAS Data series on material properties, 1–4. ASM International; 1998. p. 5.
[15] Touloukian YS. Thermal expansion: metallic elements and alloys. New York: IFI/Plenum; 1975.
[16] TMA 2940 Thermo-mechanical Analyzer Operator's Manual. TA Instruments; 1993.
[17] Certificate of Analysis, Standard Reference Material 736—Copper—Thermal Expansion, National Institute of Standards and Technology, revised October 7, 1990.
[18] Certificate of Analysis, Standard Reference Material 738—Stainless Steel (AISI 446)—Thermal Expansion, National Institute of Standards and Technology, revised November 17, 1986.
[19] Jiang N, Clum J, Chromik RR, Cotts EJ. Scripta Mater 1997;37:1851.